Proceedings Paper:

eprints@whiterose.ac.uk
https://eprints.whiterose.ac.uk/

EFFECT OF FOUR-WAY COUPLING ON THE TURBULENCE FIELD IN MULTI-PHASE CHANNEL FLOWS

L. Mortimer, M. Fairweather and D.O. Njobuenwu

School of Chemical and Process Engineering, University of Leeds, Leeds LS2 9JT, UK

pmlfm@leeds.ac.uk

Abstract

This paper investigates and compares the effect of a solid, spherical particle phase on surrounding carrier fluids (air and water) in a turbulent channel flow. The fluid phase properties are chosen to represent a flow typical of the nuclear waste industry, with the flow modelled using the direct numerical simulation (DNS) code, Nek5000, at a shear Reynolds number of 180. A Lagrangian particle tracker is developed and implemented to simulate the dispersed phase, capable of accommodating two-way coupling between the fluid and discrete phase and inter-particle collisions (four-way coupling). In order to investigate the effect that the four-way coupled particulate phase has on the turbulence field, mean fluid velocities and turbulence intensity statistics are recorded. The work demonstrates that the introduction of two-way coupling does indeed impact slightly on the turbulence field. Specifically, it reduces the mean velocity profile and increases the streamwise turbulence intensity in the near-wall region. Upon the introduction of inter-particle collisions, the flow statistics studied show a negligible response. Collision density distributions are studied and a temporal migration to the near-wall region is observed. Alongside this, to investigate particle density-ratio effects, water-based results are contrasted with simulations in air. The way in which the flow statistics are modified are shown to differ in air and water. Finally, a DLVO agglomeration model is demonstrated, whereby particles colliding with enough energy to overcome the potential barrier are considered bound. This is applied to the four-way coupled flow with temporal distributions of agglomerate counts presented.

1   Introduction

The transportation of particles through turbulent flows is of great importance and significance in many industrial environments. Aerosol manufacture, chemical engineering and mineral processing are but a few of the fields where an understanding of the flow mechanisms and properties are pertinent to the industries' overall quality and efficiency. More specifically, this work is of relevance to multi-phase nuclear waste processing and reactor coolant flows, where there exists mechanisms such as particle agglomeration which can often lead to performance impacts on the system. For instance, CRUD (Chalk River unidentified deposits), consisting of agglomerated particles, can collect upon the cladding of reactor fuel rods and is capable of reducing the efficiency of a nuclear reactor through the introduction of poor heat transfer and local corrosion.

It has previously been observed experimentally by Babler et al. (2010) that flows possessing turbulent properties are capable of encouraging particle aggregation. Simulation of particles in various flows has also been widely studied, but these are generally one-way coupled, in that they only consider the effect of the fluid on the particles. However, since the interaction between a particle and its surrounding fluid is a two-way process, it is also important to consider the effect that the dispersed-phase has on the fluid phase. Furthermore, and to carry out more realistic simulations, inter-particle collisions must also be accounted for in dense flows. DNS has been shown by Dritselis and Vlachos (2011) to be more reliable than large eddy simulation when examining the induced effects of coupling on turbulence intensities. Previous work of this nature has been carried out at high density ratios. Li et al. (2001) observed more anisotropic turbulence intensities as the particle mass loading was increased in a vertical channel flow. Furthermore, Vreman et al. (2009) offered additional qualitative descriptions surrounding the way particles affect the continuous phase at high mass loadings.

This work aims to investigate further the effect that the presence of a solid, spherical particle phase has on the carrier fluid by considering two-way and four-way coupling mechanisms at low and high density ratios. In order to relate the work to flows present in the nuclear waste industry, the properties of each phase have been chosen such that they represent a relatively high-concentration flow of particles in a viscous, liquid media such as water. This will then be compared to a flow containing the same particles by modifying the density ratio to match that of a flow in air. Finally, particle agglomeration is introduced using a DLVO (see Derjaguin and Landau (1941) and Verwey and Overbeek (1948)) potential energy barrier model to determine collisions which result in

capture. The effect that this mechanism has on the turbulence field will also be investigated.

2 Mathematical formulation

In order to obtain an accurate carrier-fluid field representing a fully developed channel flow, a direct numerical simulation was carried out. In this work the single-phase solver, Nek5000 (Fischer et al., 2008), was used which utilizes a high-order spectral element method to model the fluid phase. This software was chosen due to its parallel processing capabilities and efficiency. In the code, the incompressible Navier-Stokes equations are solved to high accuracy on a discretized Cartesian grid consisting of 27×18×23 8th order elements (i.e. 5.7M nodes), wherein the elements are scaled such that the nodes closest to the wall are distributed more densely. The Navier-Stokes equations are non-dimensionalized using the channel half-height, δ, and the bulk velocity, U_B. The computational position domain (x, y, z) corresponds to a $4\pi\delta \times 2\delta \times 2\pi\delta$ channel. Here, x is the streamwise direction, y is the wall-normal direction, and z is the spanwise direction. From here on, a quantity with an asterisk (*) denotes a variable non-dimensionalized in this manner. The flow is driven by a pressure gradient, which is maintained such that we ensure a constant mass flux and a shear Reynolds number of $Re_\tau = 180$.

For validation of the single phase, the unladen flow was compared to the recent DNS findings of Vreman and Kuerten (2014), and excellent agreement was obtained. In order to investigate average flow field sensitivity to grid resolution, the same simulation was carried out on a Kolmogorov-resolving mesh and negligible deviation was observed. For this reason, in order to reduce run times, computations were carried out on a grid which had Kolmogorov-resolving spacings at $y^+ < 40$.

In order to model particle transport, a Lagrangian particle tracker (LPT) was developed which interfaces concurrently with Nek5000. The LPT solves the non-dimensional equations of motion for each particle, Eq. (1) and (2), at timesteps equal to that of the single-phase solver. For this work, we have chosen to consider contributions from drag, lift, virtual mass and pressure gradient forces. The Basset history force has been neglected due to long computation times and previous evidence showing a lack of effect on the resulting motion. A fourth order Runge-Kutta scheme was applied for accurate integration of the differential equations in order to obtain each particle's position and velocity at every timestep. The particle properties used for all simulations are presented in Table 1.

Diameter, d_P^*	0.005
Stokes number, St	0.112
Water density ratio, ρ_P^*	2.5
Air density ratio, ρ_P^*	2041
Volume fraction, V_P/V_F	$1.16 * 10^{-4}$

Table 1: Particle properties.

Each particle's inertial effect on the fluid phase was taken into account through the inclusion of an additional source term in the Navier-Stokes equations, $f_C = \frac{1}{V} \sum_{P=1}^{N} F_P$. Here, V is the volume of a computational cell, N is the number of particles in that cell and F_P is the fluid force exerted on particle P.

The LPT also considers particle-particle interactions in the form of hard-sphere elastic collisions. At each timestep, the particles are distributed into cells within a secondary coarse mesh. The collision algorithm is then run on all of the cells in this new mesh, treating each as a new full domain. Specifically, the code determines which particles have collided by checking their relative displacements and comparing that to the sum of their radii. If the relative distance is smaller, the particles collide. This allows for fast collision detection and the resulting particle velocities/positions are then calculated, taking into account the collision-time contribution to the deflection.

$$\frac{\partial x_P^*}{\partial t^*} = u_P^* \qquad (1)$$

$$\frac{\partial u_P^*}{\partial t^*} = \underbrace{\frac{3C_D|u_s^*|}{4d_P^*\rho_P^*}u_s^*}_{Drag} + \underbrace{g^*(1-\rho^*)}_{Gravity} + \qquad (2)$$

$$\underbrace{\frac{3}{4}\frac{C_L}{\rho_P^*}(u_s^* \times \omega_F^*)}_{Lift} + \underbrace{\frac{1}{2\rho_P^*}\frac{D'u_F^*}{Dt^*}}_{Virtual\ Mass} + \underbrace{\frac{1}{\rho_P^*}\frac{Du_F^*}{Dt^*}}_{Pressure\ Gradient}$$

In order for an agglomeration event to occur, the particle's total kinetic energy must be greater than that of the energy barrier calculated using the primary maximum from the DLVO potential expression given in Eq. (3):

$$V(r) = \pi d_p \left(-\frac{H}{24\pi r} + \frac{32c_0 k_B T \gamma^2}{\kappa^2}e^{-\kappa r}\right) \qquad (3)$$

Particle statistical distributions across the wall-normal direction were obtained by splitting the domain into 32 slabs of equal size, and taking an average over all the particles in that slab. Once the particle number density near the wall had settled, particle data was collected and statistics were obtained.

The LPT was validated against the UUD group data from Marchioli et al. (2008), who simulated a particle-laden turbulent channel flow at $Re_\tau = 150$ using three different Stokes numbers. This is presented in Figure 1. Despite the difference in Reynolds number, the same qualitative response to changing the Stokes number of the particle phase is observed. Further validations have been carried out at matching Reynolds numbers and show very good agreement.
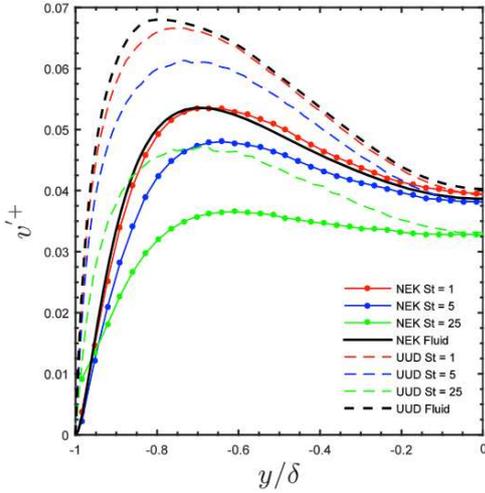
Figure 1: Spanwise RMS fluctuating velocity profiles at different Stokes numbers for qualitative validation against Marchioli et al. (2008).

3   Results and discussion

The results of coupled simulations in water are presented in Figures 2 and 3.

Figure 3: Comparison of RMS velocity profiles for two-way (top) and four-way (bottom) coupled simulations: — coupled water phase; - - - unladen water phase; ⋯ particle phase.

In these figures, the upper plots depict the response of the fluid phase to two-way coupling. Noting the slight differences between the unladen flow and the continuous (two-way coupled) flow results, it is evident that the presence of this mechanism does indeed impact the system. Specifically, the mean streamwise velocity of the particles is reduced and this effect is greater towards the centreline. This is also true of the wall-normal (v'^*) and spanwise (w'^*) RMS fluctuating velocities. Conversely, upon activating two-way coupling, the streamwise RMS (u'^*) has a higher peak and is also slightly greater at the centre-line.

The lower plots demonstrate the effects of including both two-way coupling and interparticle collisions (four-way coupling). It is notable that these resemble the two-way plots, yet there are very slight differences. The lack of response to collisions may be explicable by the particle concentration lying on the very boundary between dense and dilute volume fractions, and it is expected that we would see more of a reaction if the particle concentration were to be increased. An
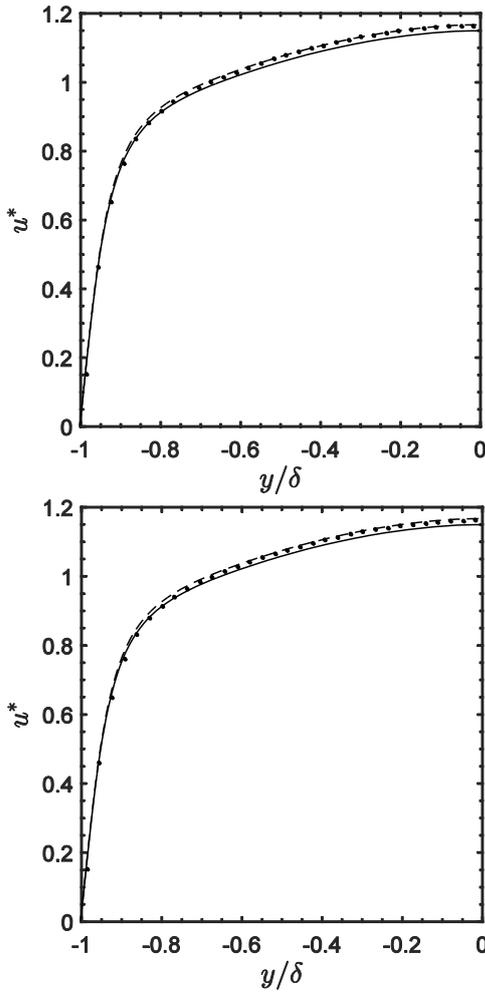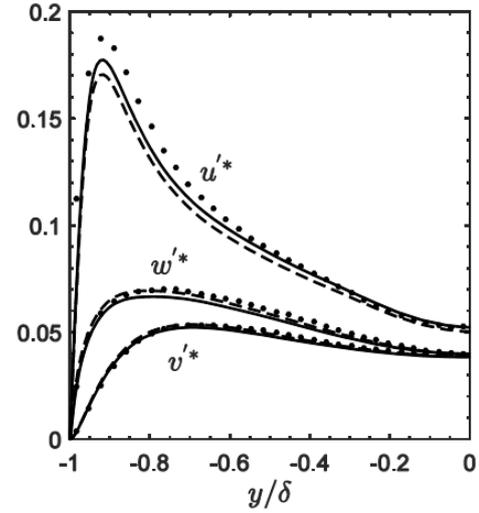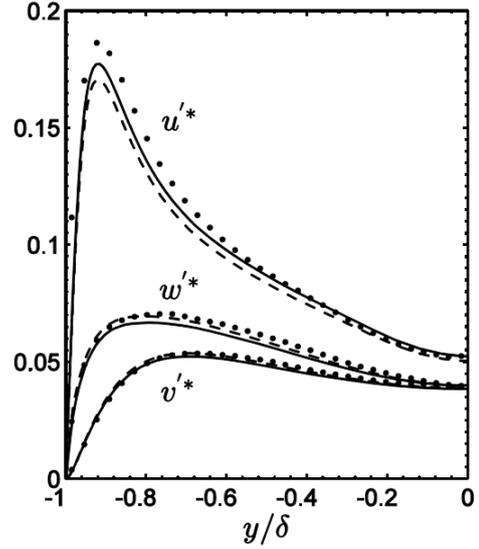

Figure 2: Comparison of mean streamwise velocity profiles for two-way (top) and four-way (bottom) coupled simulations: — coupled water phase; - - - unladen water phase; ⋯ particle phase.

increase in streamwise turbulence levels and a reduction in the other directions due to four-way coupling has been previously observed by Vreman et al. (2009). Their simulation, however, was carried out at a higher density ratio and volume fraction, and the effect was exhibited with much greater intensity.

Figures 4 and 5 illustrate the same set of simulations at a higher density ratio, matching that of particles in air.
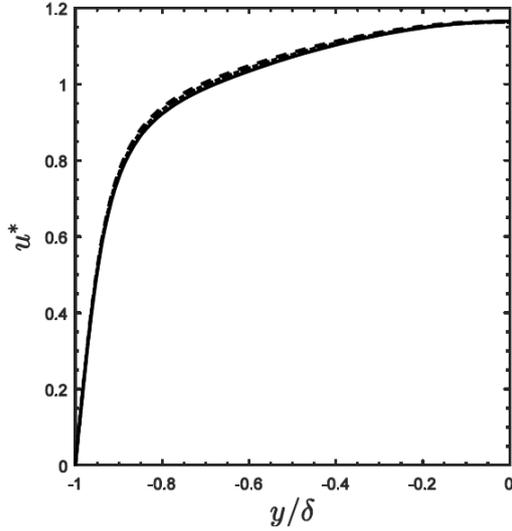

Figure 4: Comparison of coupled mean streamwise velocity profiles in air: — one-way; - - - two-way; ----- four-way.
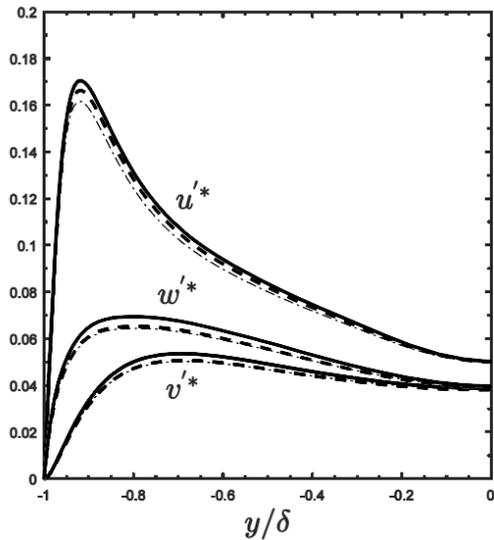

Figure 5: Comparison of coupled RMS velocity profiles in air. Legend as Figure 4.

Other than a slight increase, Figure 4 illustrates a negligible response to two- and four-way coupling when considering the mean streamwise velocity profile in air at the volume fraction investigated. In Figure 5, all three components of the RMS velocities are reduced as a result of coupling the particles with the continuous phase. For the mean streamwise velocity, the inclusion of particle collisions dampens the turbulence

further, which is in contradiction to what is observed in water (Figure 3). It was also observed that the collisions have a greater effect on this statistic than solely the coupling. The average momentum change per collision along the channel was also studied, with an increase in turbophoretic effects observed.

The average drag force per particle in both the four-way coupled air and water simulations was recorded and is presented in Figures 6 and 7. Other forces were monitored, however, drag forces were observed to have the greatest impact on the motion of the particulate phase and so will be discussed here.
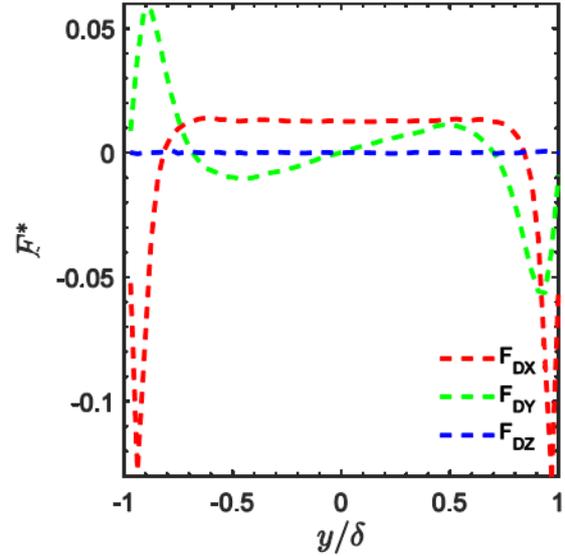

Figure 6: Average non-dimensionalized drag force components per particle across the water channel.
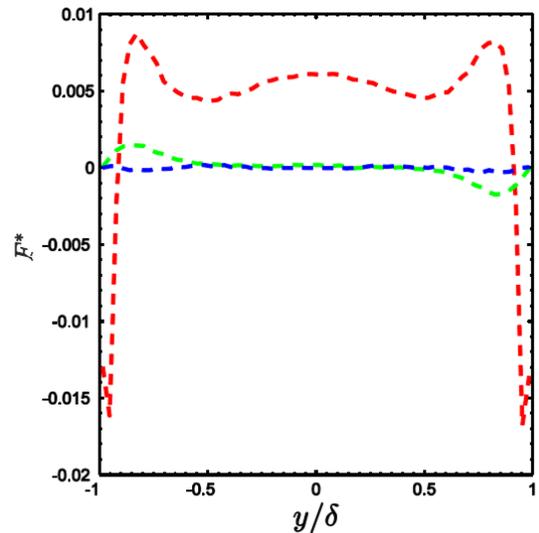

Figure 7: Average non-dimensionalized drag force components per particle across the air channel. Legend as in Figure 6.

The streamwise force in water is generally homogeneous in the bulk of the channel. In the turbulent region, the magnitude peaks and is negative. The wall-normal drag force varies across the channel. In the bulk, the particles are carried away toward the turbulent region. A pair of stable fixed points in the wall-normal force plot are observed at $y^* = \pm0.7$. Past these points, the particles are subject to high forces in all directions aside from spanwise, which is a result of the chaotic fluid velocities in that region. The average spanwise forces are negligible, which implies that they are instantaneously also very low (due to the very small fluid velocities in that direction).

Figure 7 depicts the average drag force per particle across the channel for air. In contrast with water, the forces are generally much lower, due to the inverse scaling with the density ratio. The streamwise force now deviates even in the bulk flow region, and the depth of the channel where the particles are subject to large forces downstream is much greater. In the wall-normal direction, the force is only relevant in the turbulent region and is still small compared to the upstream drag. Again, this component tends to push the particles back towards the bulk.

Comparing Figures 6 and 7 with their corresponding four-way coupled RMS velocity profiles, the effect that the drag force has on the carrier fluid is clear. The difference between the positive (air) and negative (water) turbulent region forces may explain the inconsistent behaviour seen in the streamwise RMS velocity profiles. This should be investigated in more detail at higher volume fractions.
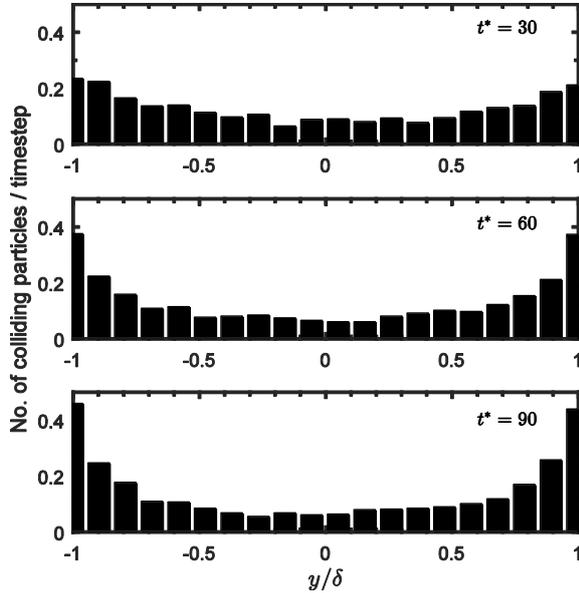

Figure 8: Temporal evolution of the number of particles likely to collide per timestep across the water channel.

Figure 8 demonstrates the time evolution of collision frequencies across the wall-normal direction in water. To obtain this plot, the near-wall particle concentration profile was allowed to settle as described
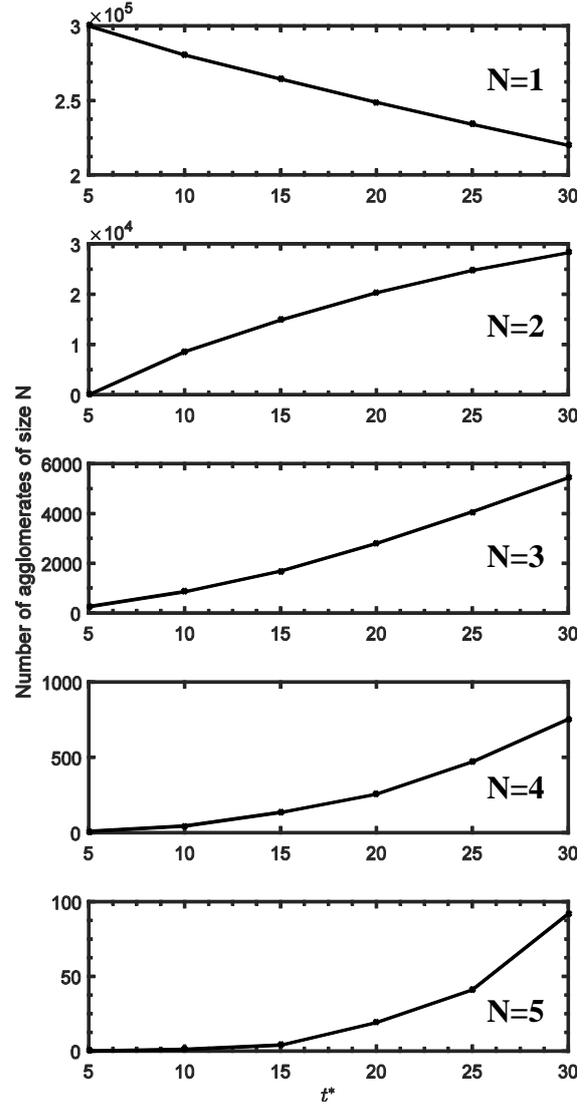

Figure 9: Number of agglomerates with N constituents as a function of time.

above. The collision mechanism was then introduced. Here, it is observed that as the particles begin to interact with each other, regions where more collisions are likely to occur migrate toward the wall. This also implies that more agglomeration events are likely to take place in those regions. Taken with the results of Figure 6, it is implied that the presence of large forces in the wall direction may be the reason for the rapid response to collisions when considering turbophoresis.

Figure 9 depicts a run using four-way coupling with the agglomeration mechanism. In order for an agglomeration event to occur, a particle must firstly collide with another. It must then possess a certain amount of kinetic energy, which is calculated using the value for the primary maximum in the DLVO equation. The resulting agglomerate is then considered as a spherical particle with twice its original volume. For an initial run, the potential was non-dimensionalized and the Hamaker constant, Debye screening length and reduced surface potential were chosen to match particles in water with arbitrary surface charge,

making sure that the potential barrier was of the order of half the average kinetic energy of the original agglomerating particles in the flow.

It is clear that it would have taken just slightly longer than the simulation time ($t^* = 30$) for $1/3$ of the particles to form agglomerates, and the number of agglomerates formed per second appears linear in this period. The rate at which $N = 2$ agglomerates are formed decreases over time, with a fairly sharp increase during the first third of the simulation. The higher order agglomerates actually accelerate in formation over time, however, their overall totals remain few. With the addition of this mechanism, and for the duration of simulation time studied, the particle statistics did not change, implying that their concentration was mostly unaffected, but further studies are required to verify this.

4   Conclusions

This work has considered the effect that two-way and four-way coupling has on the turbulence statistics associated with a multi-phase channel flow at a shear Reynolds number of 180. Direct numerical simulations have been carried out at two particle-fluid density ratios, corresponding to that of water and air. Throughout, we have demonstrated that the introduction of two- and four-way coupling does indeed modify the turbulence properties of the system.

In water, it works to reduce the overall mean velocity profile and increases the streamwise turbulence intensity in the wall-region. The inclusion of interparticle collisions has little effect on any of the statistics studied, but we do observe a temporal migration of the high collision density regions toward the wall.

In air, a qualitative difference is identified wherein the inclusion of coupling reduces the turbulence intensities in the streamwise direction. An argument to explain this involving average drag force information across the channel has been offered. It is also observed that the inclusion of particle collisions has a greater impact on this statistic. The other statistics gathered exhibit the same behaviour as in water, albeit less pronounced.

Drag forces have been examined in both systems and their qualitative properties have been discussed in all directions. It is shown that there is a much greater turbophoretic force in the water system which is barely present in air. The bulk streamwise drag force is also much larger in air. Spanwise forces are negligible in both systems.

The agglomerating flow in water studied exhibited reasonable agglomerate formation in the time simulated, however, the turbulence statistics were unresponsive to the introduction of this mechanism and so more work should be carried out to determine the influence of agglomeration on the flow field.

In future, we aim to investigate the result of increasing the concentration of the particulate phase, in an effort to encourage a more direct effect on the fluid characteristics.

References

Bäbler, U.M., Moussa, S.A., Soos, M. and Morbidelli, M. (2010), Structure and kinetics of shear aggregation in turbulent flows. I. Early stage of aggregation, Langmuir, Vol. 26, pp. 13142-13152.

Derjaguin, B.V. and Landau, L. (1941), Theory of the stability of strongly charged lyophobic sols and of the adhesion of strongly charged particles in solutions of electrolytes, Acta Physicochim. URSS, Vol. 14, pp. 633-662.

Dritselis, C. D. and Vlachos, N. S. (2011), Large eddy simulation of gas-particle turbulent channel flow with momentum exchange between the phases, Int. J. Multiphase Flow , Vol. 37, pp. 706-721.

Fischer, P.F., Lottes, J.W. and Kerkemeier, S.G. (2008), Nek5000, http://nek5000.mcs.anl.gov.

Li, Y., McLaughlin, J.B., Kontomaris, K. and Portela, L. (2001), Numerical simulation of particle-laden turbulent channel flow, Phys. Fluids, Vol. 3, pp. 2957-2967.

Marchioli, C., Soldati, A., Kuerten, J.G.M., Arcen, B., Taniere, A., Goldensoph, G., Squires, K.D., Cargnelutti, M.F. and Portela, L.M. (2008), Statistics of particle dispersion in direct numerical simulations of wall-bounded turbulence: Results of an international collaborative benchmark test, Int. J. Multiphase Flow, Vol. 34, pp. 879-893.

Verwey, E. J. W. and Overbeek, J. T. G. (1948), Theory of stability of lyophobic colloids, Elsevier Amsterdam.

Vreman, A.W. and Kuerten, J. G. M. (2014), Comparison of direct numerical simulation databases of turbulent channel flow at $Re_\tau = 180$, Phys. Fluids, Vol. 26, 015102.

Vreman, B., Geurts, B.J., Deen, N.G., Kuipers, J.A.M. and Kuerten, J.G.M. (2009), Two- and four-way coupled Euler-Lagrangian large-eddy simulation of turbulent particle-laden channel flow, Flow, Turbul. Combust., Vol. 82, pp. 47-71.